Supplement of Atmos. Chem. Phys., 15, 6247–6270, 2015
http://www.atmos-chem-phys.net/15/6247/2015/
doi:10.5194/acp-15-6247-2015-supplement

Atmospheric Chemistry and Physics Open Access

Supplement of

Sources, transport and deposition of iron in the global atmosphere

R. Wang et al.

Correspondence to: R. Wang (rong.wang@lsce.ipsl.fr)

Table S1. Iron content in coal (%) by country. Sample number (N), mean, standard deviation (SD), and geometric mean (geomean) are listed. The data are compiled from the World Coal Quality Inventory (Tewalt, 2010).

Country	N	Mean	SD	Geomean
China	332	0.98	0.77	0.73
US	117	0.62	0.88	0.28
Russia	12	0.79	1.25	0.36
Mongolia	37	0.76	0.73	0.53
Kazakhstan	18	0.54	0.53	0.34
Japan	2	0.60	0.02	0.60
South Korea	11	0.58	0.51	0.41
North Korea	50	0.87	0.72	0.65
Philippines	6	0.76	0.41	0.69
Vietnam	6	0.69	0.52	0.46
Thailand	23	1.82	1.80	1.12
India	4	2.43	1.05	2.29
Indonesia	8	0.60	0.43	0.48
Malaysia	2	0.80	0.14	0.79
Australia	10	0.46	0.30	0.38
Afghanistan	118	2.36	4.35	1.09
Iran	57	1.36	0.97	1.01
Turkey	71	2.94	1.65	2.48
Egypt	23	3.29	2.70	2.48
Georgia	1	1.02	-	1.02
Ukraine	33	1.67	1.51	0.88
Norway	27	1.13	2.63	0.55
Slovak Republic	8	0.93	0.71	0.76
Romania	12	1.07	1.02	0.77
Serbia	5	1.55	1.49	1.03
Greece	2	2.24	0.04	2.23
France	3	0.40	0.02	0.40
Spain	10	1.34	0.60	1.18
Belgium	10	0.74	0.63	0.51
United Kingdom	77	1.39	1.49	0.95
Nigeria	22	1.28	2.08	0.46
Tanzania	24	1.12	0.90	0.85
Zambia	14	2.07	3.35	0.85
Zimbabwe	6	0.25	0.29	0.12
Botswana	17	1.41	0.75	1.22
South Africa	40	0.54	0.34	0.41
Canada	12	0.98	0.51	0.88
Mexico	1	1.47	-	1.47
Brazil	63	3.47	2.92	2.51
Venezuela	16	0.86	1.28	0.28
Colombia	16	0.46	0.93	0.18
Peru	16	0.55	0.57	0.34
Chile	23	1.20	1.17	0.86
Argentina	7	6.01	13.89	1.28
New Zealand	7	0.59	0.36	0.40

Table S2. Information for the observed Fe concentrations in the air close to the land surface collected in the literature.

Region	Period	Start month	End month	Lat	Lon	Size	Fe conc, ng m^{-3}	Reference
Fuzhou	2007	4	5	26.08	119.30	$PM_{2.5}$	1115	Xu et al., 2012
Fuzhou	2007	9	9	26.08	119.30	$PM_{2.5}$	219	Xu et al., 2012
Fuzhou	2007	11	11	26.08	119.30	$PM_{2.5}$	723	Xu et al., 2012
Fuzhou	2007	1	1	26.08	119.30	$PM_{2.5}$	563	Xu et al., 2012
Shanghai	1999-2000	1	12	31.20	121.40	$PM_{2.5}$	900	Ye et al., 2003
Hangzhou	2001-2002	1	12	30.20	120.10	PM_{10}	2190	Cao et al., 2009
Beijing	2001-2003	1	12	39.90	116.40	PM_{10}	5500	Okuda, et al. 2004
Beijing	2002-2003	6	8	39.90	116.40	PM_{10}	3730	Sun et al., 2004
Beijing	2002-2003	1	1	39.90	116.40	PM_{10}	2620	Sun et al., 2004
Yong'an	2007	4	4	25.97	117.36	$PM_{2.5}$	736	Yin et al., 2012
Yong'an	2007	11	11	25.97	117.36	$PM_{2.5}$	930	Yin et al., 2012
Yong'an	2007	1	1	25.97	117.36	$PM_{2.5}$	582	Yin et al., 2012
Chengdu	2009	4	4	30.66	104.00	$PM_{2.5}$	4850	Tao et al., 2013
Chengdu	2009	5	5	30.66	104.00	$PM_{2.5}$	892	Tao et al., 2013
Jinan	2006-2007	3	5	36.67	117.03	$PM_{2.5}$	1940	Yang et al., 2012
Jinan	2006-2007	6	8	36.67	117.03	$PM_{2.5}$	990	Yang et al., 2012
Jinan	2006-2007	9	11	36.67	117.03	$PM_{2.5}$	1610	Yang et al., 2012
Jinan	2006-2007	1	2	36.67	117.03	$PM_{2.5}$	2020	Yang et al., 2012
Mt. Yulong	2010	1	2	27.42	100.13	TSP	1258	Zhang, et al., 2012
Beijing	2000	1	12	39.80	116.47	$PM_{2.5}$	1150	Yang et al., 2005
Shanghai	2000	1	12	31.23	121.32	$PM_{2.5}$	820	Yang et al., 2005
Zhengzhou	2010	3	5	34.80	113.52	$PM_{2.5}$	1896	Geng et al., 2013
Zhengzhou	2010	6	8	34.80	113.52	$PM_{2.5}$	370	Geng et al., 2013
Zhengzhou	2010	9	11	34.80	113.52	$PM_{2.5}$	1068	Geng et al., 2013
Zhengzhou	2010	1	2	34.80	113.52	$PM_{2.5}$	1435	Geng et al., 2013
Lijiang	2009	3	5	27.42	100.13	TSP	510	Zhang et al., 2013.
Hongkong	2001	1	1	22.3	114.2	PM_{10}	701	Cohen,2004
Cheju	2008	4	4	33.28	126.17	TSP	500	Kim et al., 2013
Cheju	2008	7	7	33.28	126.17	TSP	120	Kim et al., 2013
Cheju	2008	10	10	33.28	126.17	TSP	200	Kim et al., 2013
Cheju	2008	1	1	33.28	126.17	TSP	130	Kim et al., 2013
East China Sea	2005-2007	3	4	25.08	123.2	TSP	410	Hsu et al., 2010

Figure S1. Frequency distribution of Fe contents in coal (a-c), wood (d), grass (e) and crop residue (f). The number of samples (n) and the mean and standard deviation (SD) of log_{10}-transformed Fe content are shown in each panel. The x-axis is plotted on a log scale.

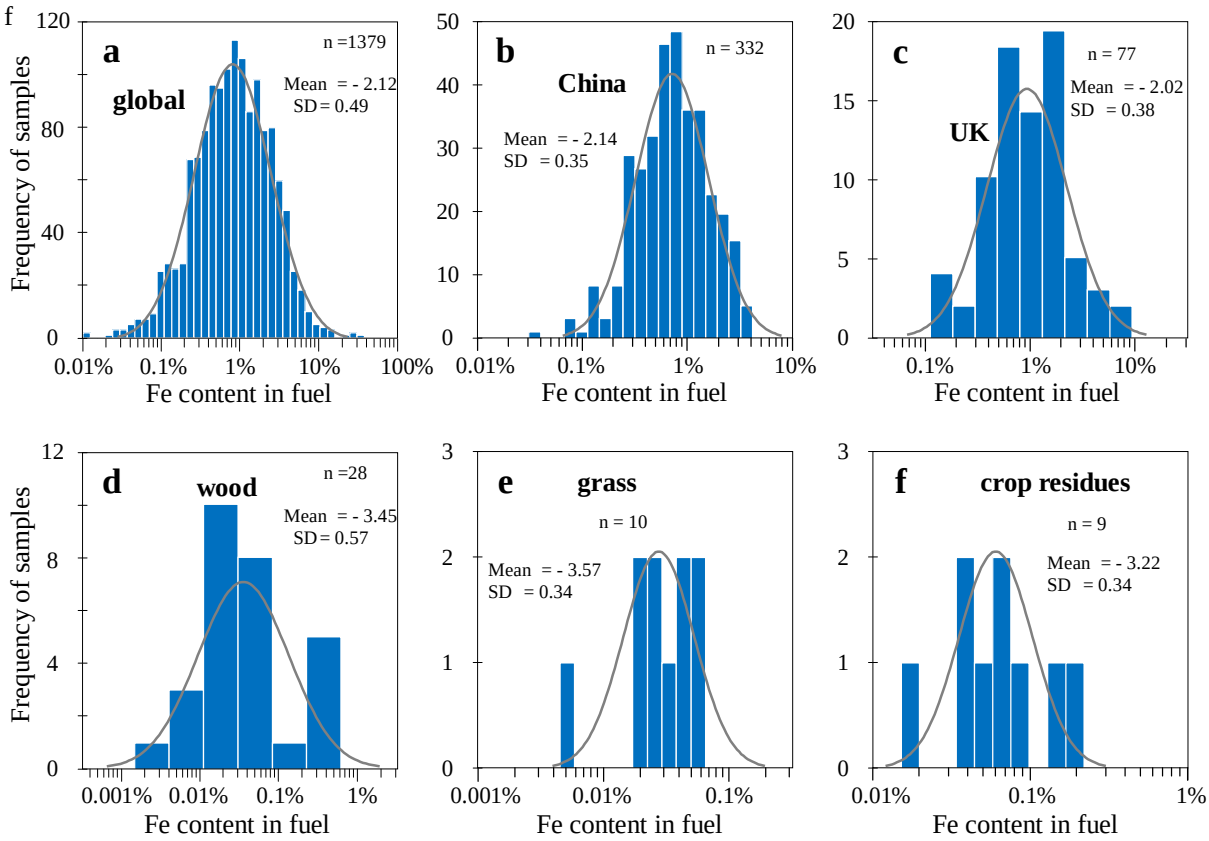

Figure S2. Iron content in clay (A) and silt (B) size particles in surface soil (CASE 2) derived from the mineralogical data set by Journet et al. (2014).

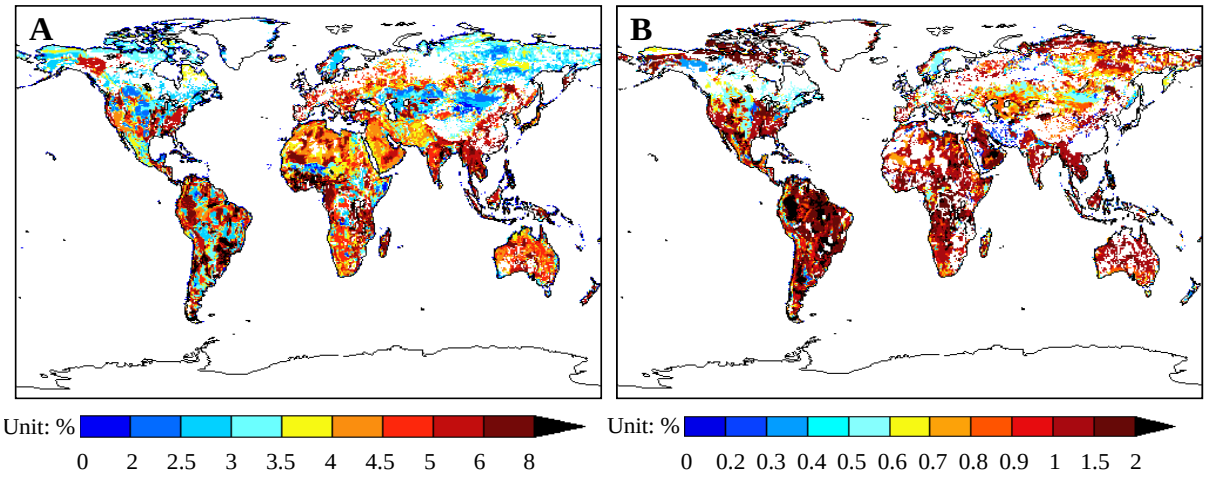

Figure S3. Maps of Fe emissions from all combustion sources at a resolution of 0.5 °×0.5 ° at 10-year intervals for 1960–2000 and for 2007. Unit: mg m^{-3} yr^{-1}.

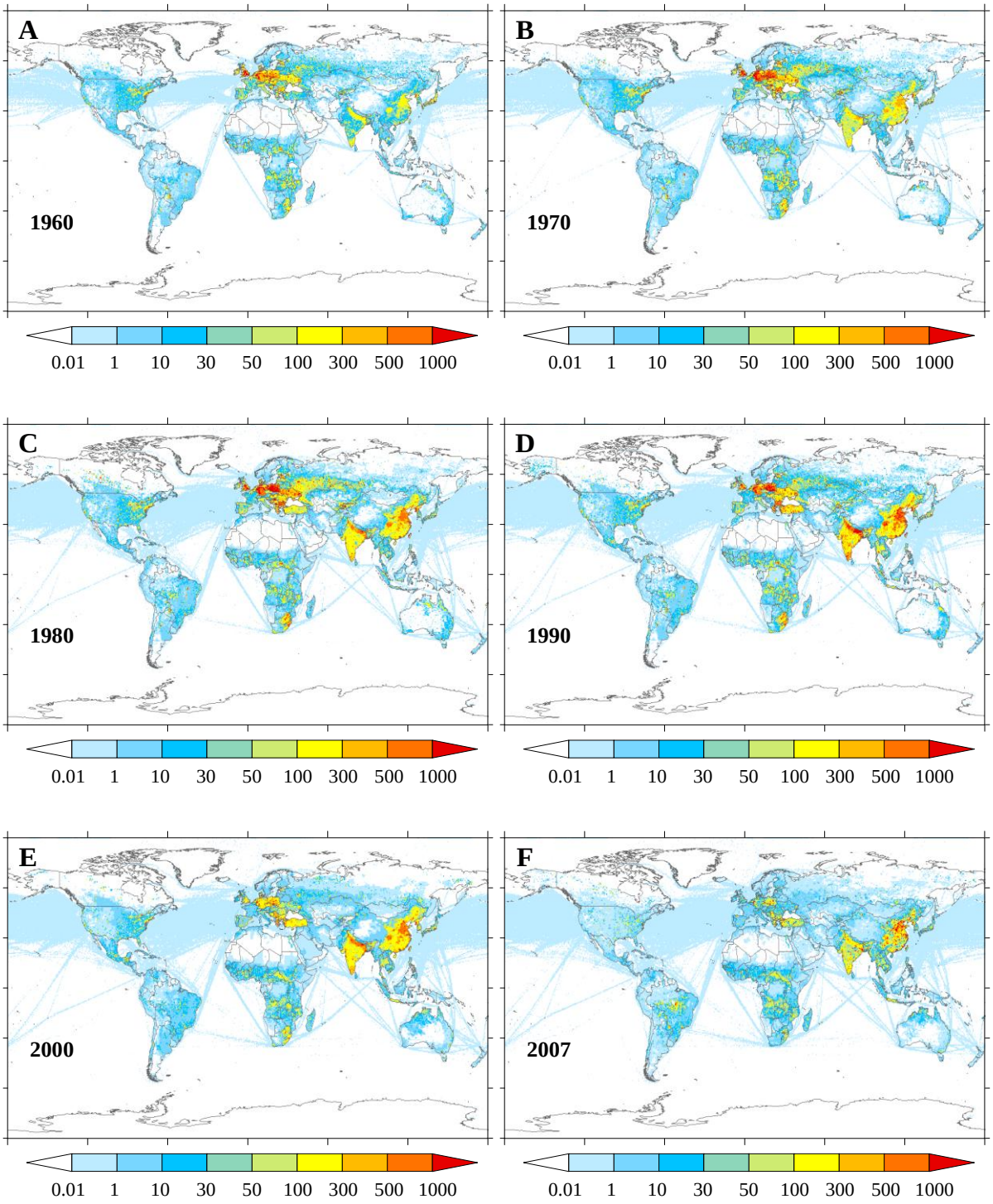

Figure S4. Global distribution of Fe content in dust simulated by assuming that Fe content of emitted dust is equal to that in the clay fraction of soil. The Banizoumbou ground-based site where Formenti et al. (2014) measured the composition of dust is shown as a blue pentagram.

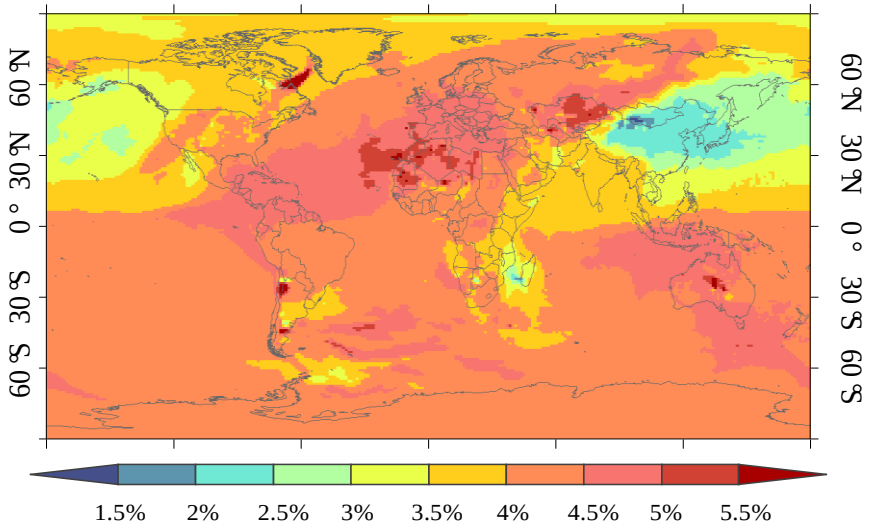

Figure S5. Comparisons of modelled and measured Fe concentrations attached to aerosols in surface air with (A) or without (B) applying a temporal scaling for the Fe concentrations from combustion based on the temporal change of the emissions. The four groups (G1, G2, G3 and G4) are the same as that shown in Fig. 12 in the main text based on the contribution of combustion to Fe concentrations: G1, contribution $\geqslant$ 50% (blue triangles); G2, 30% $\leqslant$ contribution <50% (red triangles); G3: 15% $\leqslant$ contribution <30% (green triangles); G4, contribution <15% (grey squares). The ratios between measured and modelled concentrations as geometric means are listed with the number of stations in the brackets for each group. The fitted curves for the G1 stations are shown as blue lines with coefficients of determination (r^2).

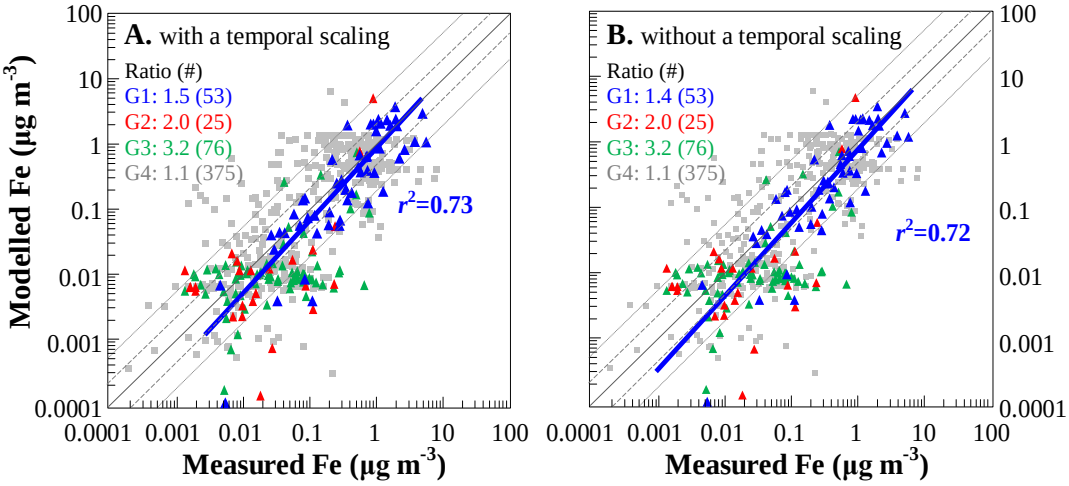

Figure S6. Zonal distribution of the modelled (blue) and observed (red) Fe concentrations over the Atlantic Ocean from 70 ℃S to 60 ℃N. The modelled Fe concentrations were derived with (model 1) or without (model 2) using the new mineralogy data. Error bars show the geometric standard deviations of Fe concentrations at all sites in each region.

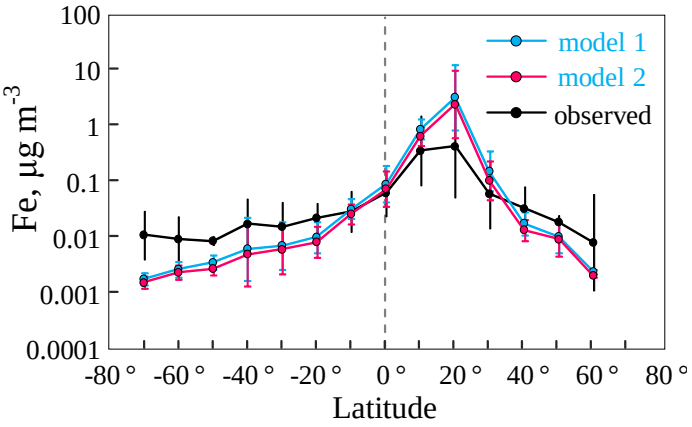

Figure S7. Plot of modelled and observed deposition rates of Fe. The fitted curve of all data points is shown as a black dashed line with coefficient of determination (r^2).

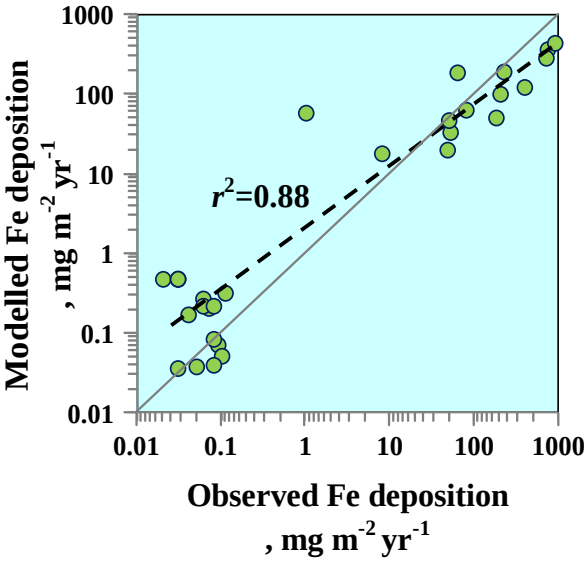

References

1. Cao, J., Shen, Z., Chow, J. C., Qi, G. W., and Watson, J. G.: Seasonal variations and sources of mass and chemical composition for PM10 aerosol in Hangzhou, China, Particuology, 7(3), 161-168, 2009

2. Cohen, D. D., Garton, D., Stelcer, E., Hawas, O., Wang, T., Poon, S., Kim, J., Choi, B. C., Nam Oh, S., Shin, H. J., Ko, M. Y., and Uematsu, M.: Multielemental analysis and characterization of fine aerosols at several key ACE-Asia sites, J. Geophys. Res., 109(D19), doi: 10.1029/2003JD003569, 2004.

3. Geng, N., Wang, J., Xu, Y., Zhang, W., Chen, C., and Zhang, R.: $PM_{2.5}$ in an industrial district of Zhengzhou, China: Chemical composition and source apportionment, Particuology, 11(1), 99-109, 2013.

4. Formenti, P., Caquineau, S., Desboeufs, K., Klaver, A., Chevaillier, S., Journet, E., and Rajot, J. L.: Mapping the physico-chemical properties of mineral dust in western Africa: mineralogical composition, Atmos. Chem. Phys., 14, 10663–10686, doi:10.5194/acp-14-10663-2014, 2014.

5. Hsu, S. C., Wong, G. T. F., Gong, G. C., Shiah, F. K., Huang, Y. T., Kao, S. J., Tsai, F., Lung, S. C., Lin F. J., Lin, I., Huang, C., and Tseng, C.: Sources, solubility, and dry deposition of aerosol trace elements over the East China Sea, Mar. Chem., 120(1), 116-127, 2010.

6. Journet, E., Balkanski, Y., and Harrison, S. P.: A new data set of soil mineralogy for dust-cycle modeling, Atmos. Chem. Phys., 14(8), 3801-3816, 2014.

7. Kim, W. H., Hwang, E. Y., Ko, H. J., and Kang, C. H.: Seasonal Composition Characteristics of TSP and $PM_{2.5}$ Aerosols at Gosan Site of Jeju Island, Korea during 2008-2011. Asian J. Atmos. Environ., 7(4), 217-226, 2013.

8. Okuda, T., Kato, J., Mori, J., Tenmoku, M., Suda, Y., Tanaka, S., He, K., Ma, Y., Yang, F., Yu, X., Duan, F., and Lei, Y.: Daily concentrations of trace metals in aerosols in Beijing, China, determined by using inductively coupled plasma mass spectrometry equipped with laser ablation analysis, and source identification of aerosols. Sci. Total Environ., 330(1), 145-158, 2004.

9. Sun, Y., Zhuang, G., Wang, Y., Han, L., Guo, J., Dan, M., Zhang, W., Wang, Z., and Hao, Z.: The air-borne particulate pollution in Beijing-concentration, composition, distribution and sources. Atmos. Environ., 38(35), 5991-6004, 2004.

10. Tao, J., Zhang, L., Engling, G., Zhang, R., Yang, Y., Cao, J., Zhu, C., Wang, Q., and Luo, L.: Chemical composition of $PM_{2.5}$ in an urban environment in Chengdu, China: Importance of springtime dust storms and biomass burning. Atmos. Res., 122, 270-283, 2013.

11. Tewalt, S.J., Belkin, H.E., SanFilipo, J.R., Merrill, M.D., Palmer, C.A., Warwick, P.D., Karlsen, A.W., Finkelman, R.B., and Park, A.J.: Chemical analyses in the World Coal Quality Inventory, version 1: U.S. Geological Survey Open-File Report 2010-1196, http://pubs.usgs.gov/of/2010/1196/, 2010.

12. Xu, L., Chen, X., Chen, J., Zhang, F., He, C., Zhao, J., and Yin, L.: Seasonal variations and chemical compositions of $PM_{2.5}$ aerosol in the urban area of Fuzhou, China, Atmos. Res., 104, 264-272, 2012.

13. Yang, F., Ye, B., He, K., Ma, Y., Cadle, S., Chan, T., and Mulawa, P. A: Characterization of Atmospheric Mineral Components of $PM_{2.5}$ in Beijing and Shanghai, China, Sci. Total Environ., 343(1), 221-230, 2005.

14. Yang, L., Zhou, X., Wang, Z., Zhou, Y., Cheng, S., Xu, P., Gao, X., Nie, W., Wang, X., and Wang, W.: Airborne fine particulate pollution in Jinan, China: concentrations, chemical compositions and influence on

visibility impairment. Atmo. Environ., 55, 506-514, 2012.

15. Ye, B., Ji, X., Yang, H., Yao, X., Chan, C., Cadle, S., Chan, T., and Mulawa, P.: Concentration and chemical composition of $PM_{2.5}$ in Shanghai for a 1-year period, Atmos. Environ., 37(4), 499-510, 2003.
16. Yin, L., Niu, Z., Chen, X., Chen, J., Xu, L., and Zhang, F.: Chemical compositions of $PM_{2.5}$ aerosol during haze periods in the mountainous city of Yong'an, China. J. Environ. Sci., 24(7), 1225-1233, 2012.
17. Zhang, N., Cao, J., Ho, K., and He, Y.: Chemical characterization of aerosol collected at Mt. Yulong in wintertime on the southeastern Tibetan Plateau. Atmos. Res., 107, 76-85, 2012.
18. Zhang, N., Cao, J., Xu, H., and Zhu, C.: Elemental compositions of $PM_{2.5}$ and TSP in Lijiang, southeastern edge of Tibetan Plateau during pre-monsoon period. Particuology, 11(1), 63-69, 2013.